Effect of Heavy-Ion Irradiation on the Gas Permeability of Poly(ethylene terephthalate) (PET) Membranes

SHUICHI TAKAHASHI,[1] MASARU YOSHIDA,[2] MASAHARU ASANO,[2] TOMOHIRO TANAKA,[1] TSUTOMU NAKAGAWA[1]

[1] Department of Industrial Chemistry, Meiji University, Higashi-mita, Tama-ku, Kawasaki 214-8571, Japan

[2] Department of Material Development, Takasaki Radiation Chemistry Research Establishment, Japan Atomic Energy Research Institute, 1233 Watanuki-Machi, Takasaki 370-1207, Japan

Received 11 October 2000; accepted 5 January 2001

ABSTRACT: A poly(ethylene terephthalate) (PET) membrane was used to study the effect of heavy-ion irradiation on gas permeability and selectivity. In an ambient temperature range of 303–333 K, permeability coefficients for He, N_2, O_2, and CO_2 were determined with the vacuum-pressure and time-lag methods. Gas-permeability coefficients of the membranes, which were irradiated with some specific heavy ions, increased remarkably without a significant change in the polymer structure by ion irradiation. The permeation rates of these membranes were inversely proportional to the square root of the molecular weight of the gasses and showed Knudsen flow because of the formation of pores caused by heavy-ion irradiation. © 2001 John Wiley & Sons, Inc. J Appl Polym Sci 82: 206–216, 2001

Key words: heavy-ion irradiation; gas permeability; separation factor; activation energy; Knudsen flow

INTRODUCTION

Recently, there has been growing interest in the heavy-ion irradiation of polymer membranes. Heavy-ion irradiation often causes different chemical effects as a result of γ-ray or electron-ray irradiation.[1–6] Energetic heavy ions are ionizing particles that create zones of high-density excitations and ionizations as they pass through membrane materials and cause many effects due to the high local dose within the ion tracks. These damage zones are called *latent tracks*, and they are greater than those caused by γ-rays or electron rays.[7–9] In addition, it has been proven that an interaction occurs between heavy ions and polymer materials in which the degree of damage to the polymer material differs with the kind of ions irradiated.[10–13] It is possible that ion-irradiated membranes of poly(ethylene terephthalate) (PET), a copolymer of diethyleneglycol-bis-allylcarbonate, polycarbonate, and cellulose nitrate, form cylindrical pores by etching with an aqueous solution of strong alkali.[7–10] Particularly, the mechanical strength of PET is high, and it seems to be the optimum material to easily undergo various chemical changes by the ion irradiation. In addition, it is impossible to form cylindrical pores in polyethylene (PE) and polytetrafluoroethylene by irradiation. The pores formed by etching can be observed by scanning electron microscopy (SEM). The presence of pores cannot be confirmed by SEM or transmission electron microscopy without etching after irradiation. Furthermore, it

Correspondence to: T. Nakagawa (nakagawa@isc.meiji.ac.jp).

Journal of Applied Polymer Science, Vol. 82, 206–216 (2001)
© 2001 John Wiley & Sons, Inc.

has also been found that the potential for the damage of polymer materials differs with the kinds and energy of ions irradiated. Generally, the depth of ion penetration tends to increase with the decrease in the atomic number of the irradiated ion. Also, the dimensions of the damage tend to increase with the increase in atomic number of the irradiated ion. It is considered that the damage is caused by the energy and size of irradiated ions. Before ion irradiation, the size (atomic radius) of the atoms of irradiated ions in this study were as follows: Xe = 2.20 Å, Kr = 2.01 Å, Ar = 1.91 Å, Ne = 1.59 Å, and N = 0.53 Å. Therefore, the order of ion size was as follows: Xe > Kr > Ar > Ne > N.

In recent years, heavy-ion irradiation has been utilized and studied in many fields, including nuclear fusion, medicine, materials technology, and other scientific fields. For example, Yoshida et al. reported the first successful synthesis of a novel thin film with a pore structure that opened and closed in aqueous solution depending on the temperature.[14] Tamada et al. reported the thermal response of ion-track pores in various copolymer films.[15]

In this study, heavy-ion irradiation was utilized for the modification of membranes. The effect of irradiation by various heavy ions on the gas permeability of PET membranes was investigated. PET is a polymer that is widely used for fibers, films, and bottles. It was assumed that for PET, which is often used as a gas-barrier film, it would be easy to effect changes in its gas permeability by modifications, such as ion irradiation. We also examined the possibility of controlling gas permeability by ion irradiation. So far, the study of the gas permeability of heavy-ion-irradiated membranes has not been reported.

EXPERIMENTAL

Material

The PET membranes used in this study were obtained from Toppan Printing Co., Ltd. (Tokyo, Japan). The thickness of the PET membranes was 12 μm.

Heavy-Ion Particle Irradiation

For heavy-ion particle irradiation, a PET membrane of 12 μm was cut into a 40 × 40-mm square and then attached to a 50 × 50 × 1-mm glass plate.

The chamber for the formation of ion-track pores in the membrane, which was connected with the azimuthally varying field (AVF) cyclotron in the Takasaki ion accelerators for advanced radiation applications (TIARA), Japan Atomic Energy Research Institute (Gunma, Japan), was new and was designed for the alternate use of turntable-type and roll-type film-carrying systems. The schematic representation of this chamber is illustrated in Figure 1. The ion beam from the AVF cyclotron was followed, and the geometry and distribution of the ion beam in the neighborhood of the target holders were measured by both the three-wire profile monitor (Irie Co., Ltd., Tokyo, Japan) and a charge-coupled device camera connected with an alumina monitor. The widespread occurrence of ions was controlled by a combination of defocusing with a quadruple electromagnet and collision with metal foils, such as Al, Ta, and Cu, for scattering. The turntable-type film-carrying system could irradiate the six square films (40 × 40 mm) by rotation of the turntable. The roll-type film-carrying system, which could irradiate the 100 mm wide film at the maximum by the combined use of a widespread occurrence and a scanning mechanism.

For ion-beam irradiation, $^{15}N^{3+}$(56MeV), $^{20}Ne^{4+}$ (75MeV), $^{40}Ar^{8+}$(150MeV), $^{84}Kr^{17+}$ (150MeV) and $^{129}Xe^{23+}$ (450MeV) were supplied from the AVF cyclotron, TIARA. The *fluence* (the number of irradiated ions per unit area) of ion irradiation was changed, and the effect of the fluence on the gas permeability was also confirmed. Etching with an aqueous solution of strong alkali, in this study, was not carried out after the ion irradiation.

Measurement of Membrane Characterization

The densities of all of the PET membranes was determined with an aqueous solution of calcium nitrate at room temperature. The Fourier transform infrared (FTIR) spectrometer (JASCO FT/IR–7300) was used to scan the IR spectrum of the untreated and the ion-irradiated PET membranes. The d-spacing was measured by wide-angle X-ray diffraction (WAXD; RIGAKU RINT-1200) with the Braggs equation: $\lambda = 2d \sin \theta$(Cu Kα, λ = 1.54 Å).

Gas-Permeation Properties

The gas permeability of the membranes was determined by vacuum-pressure methods.[16] The apparatus for the gas-permeation measurement is

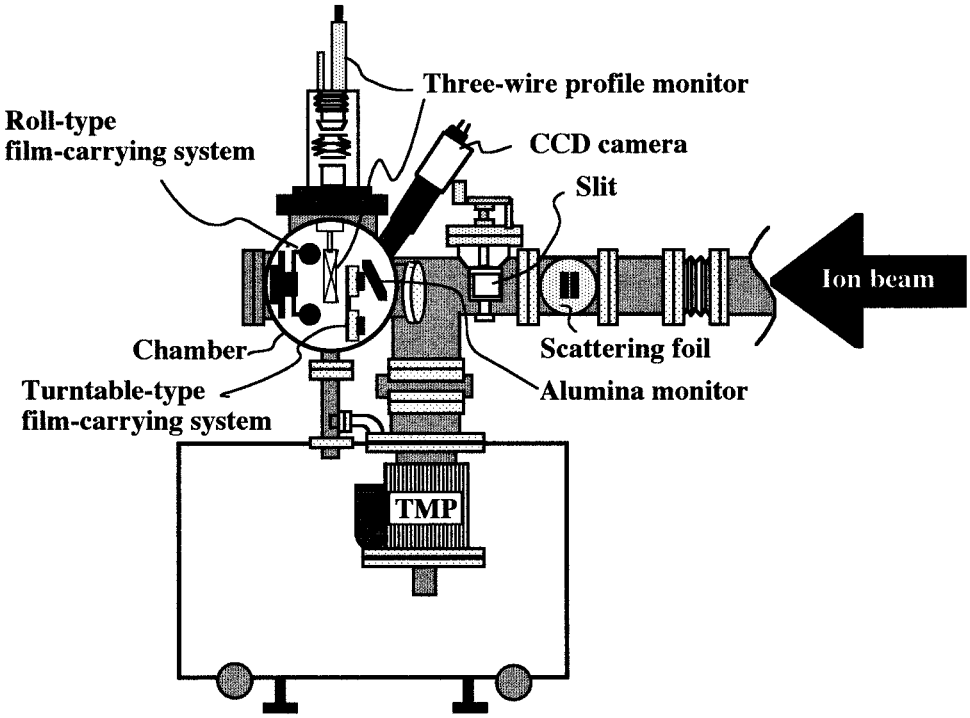

Figure 1 Schematic representation of the chamber connected with the AVF cyclotron in the TIARA.

illustrated in Figure 2. C in Figure 2 is poly(1-trimethylsilyl-1-propyne) (PTMSP) powder that adsorbs vacuum-pump oil vapor.[17,18] When an oil rotary vacuum pump was used, the effect of the oil vapor was not completely removed even though liquid nitrogen was used for the cold trap. An adsorption column filled with PTMSP powder was placed between the membrane and the cold trap as one of the countermeasures against oil-vapor contamination. The gas transport study was carried out according to the general method.[16,19,20] The permeability coefficient (P) was calculated from the slope of the time–pressure curves in the steady state. The apparent activation energy of permeation (E_p) was determined with the Arrhenius equation:[21]

$$P = P_0 \exp(-E_p/RT) \quad (1)$$

where P_0 is the preexponential factor, R is the gas constant, and T is the absolute temperature.

The ideal separation factor through the membrane was calculated with the Ps for components A and B:

$$\alpha_{A/B} = P_A/P_B \quad (2)$$

The gas-permeation measurements were carried out for pure He, N_2, O_2, and CO_2 in an ambient temperature range of 303–333 K. However, the gas-permeation measurements for a few ion-irradiated PET membranes were carried out only at 303 K. These gasses were used without further purification. Their main characteristics are given in Table I.

RESULTS AND DISCUSSION

Characterization

The d-spacing and density of the untreated PET membrane and heavy-ion-irradiated PET membranes are shown in Table II. The d-spacing, density, and FTIR spectrum did not show much difference between the untreated PET membrane and all of the irradiated PET membranes. Hama et al. investigated the effects of heavy-ion-beam irradiation on a thick slab of low-density PE by micro-FTIR measurement.[22] They observed the presence of *trans*-vinylene, carbonyl, and hydroxyl groups in ion-beam-irradiated PE film. In this study, however, these chemical structural

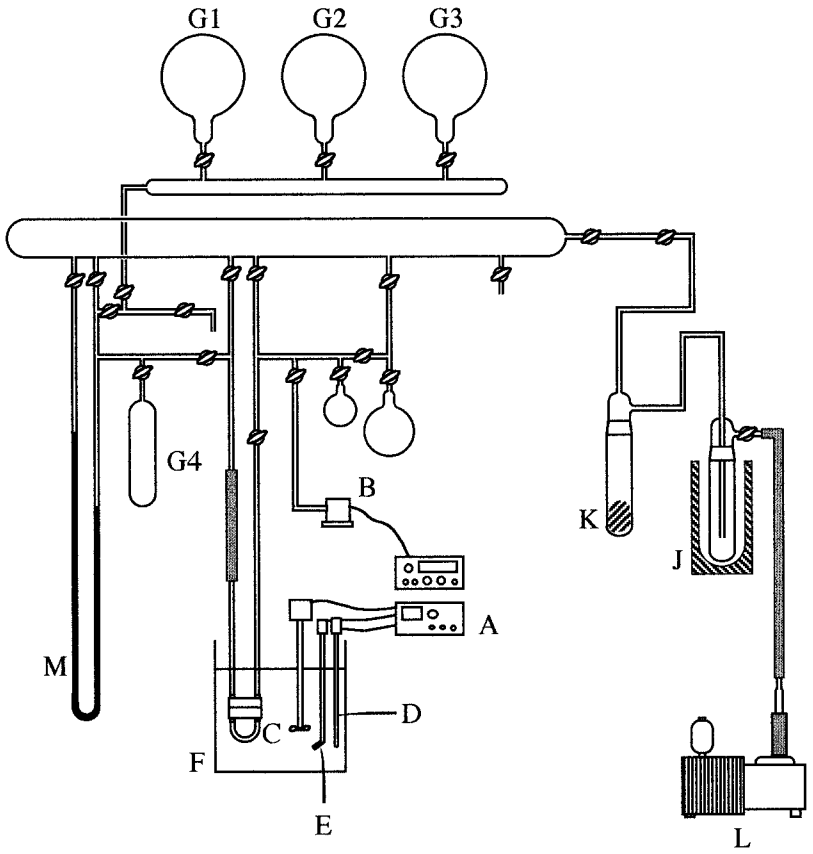

Figure 2 Schematic illustration of the apparatus for the gas-permeation measurements: (A) transistor relay, (B) pressure transducer (MKS Baratoron 270, MKS Instruments, Inc., Tokyo, Japan), (C) permeation cell, (D) thermoregulator, (E) heater, (F) water bath, (G1–G4) gas reservoir, (J) cold trap, (K) PTMSP, (L) vacuum pump, and (M) manometer.

changes were impossible to detect with an FTIR spectrum.

Permeation Properties

In general, the permeability of a gas across the membrane depends on both solubility and diffusibility, which vary from a glassy polymer to a rubbery polymer. Gas dissolves into the membrane material and diffuses across it. If the membrane contains pores large enough to allow convective flow, however, separation does not occur. If the size of the pores is smaller than the mean free path of the gas molecules, these pores allow lighter molecules to preferentially diffuse through the pores. This permeation property is Knudsen flow. Moreover, if the pores are small enough, large molecules are unable to pass through them and are excluded by the membrane. This molecular sieving is potentially useful in separating molecules of different sizes. In this study, the effect of fluence and the types of irradiated ions on the gas permeation of PET membranes was investigated. It was observed that the transition between the Knudsen flow and solution–diffusion mechanism depended on the size and amount of formed pores.

Effect of Heavy-Ion Irradiation

When the fluence of ion irradiation was over 10^{13} ions/cm^2, the irradiated membranes became brit-

Table I Molecular Properties of Penetrant Gasses

Gas	Molecular Weight	Boiling Point (°C)	Critical Temperature (°C)	Critical Volume (cm^3/mol)
He	4	−268.9	−267.9	57.4
O_2	32	−183.0	−118.8	73.4
N_2	28	−195.8	−147.2	89.8
CO_2	44	−78.5	31.0	93.9

Table II Characterizations of Untreated and Heavy-Ion-Irradiated PET Membranes

Sample	Density (g/cm^3)[a]	d-spacing[b]
Untreated PET membrane	1.40	3.4
All of the irradiated PET membranes	1.39–1.40	3.4

[a] Density was determined with an aqueous solution of calcium nitrate at room temperature.
[b] d-spacing was determined by WAXD with Bragg's equation.

tle and discolored. Therefore, all gas-permeation measurements were carried out when the fluence of heavy-ion irradiation was below 10^{12} ions/cm^2. If an interaction occurred between the irradiated ions and the PET membrane, all the used ions were expected to pass through the thin PET membrane (12 μm).

The Ps at 303 K of PET and five kinds of ion-irradiated PET membranes are shown in Table III. There was no difference between PET and Ar-ion-irradiated membranes, Ar-1 and Ar-2. It was considered that the changes in permeabilities were essentially not generated by Ar-ion irradiation because the interaction between the PET membrane and Ar ions was very weak. It was probably caused by the closing of the ion track formed by the recombination of free radicals induced by irradiation. However, the change in the gas permeation of other ion-irradiated membranes was confirmed. Notably, the Ps of N-2, Ne-2, and Xe-2 were remarkably increased by heavy-ion irradiation. N and Ne ions showed higher Ps at 10^{11} ions/cm^2. As noted previously, the depth of ion penetration tended to increase with the decrease in atomic number of the irradiated ion. The ions of smaller atomic number, such as N and Ne, passed through the PET membrane of 12 μm thickness but were not able to cause heavy damage to the membrane compared with an ion of higher atomic number, such as Xe. It was assumed that the increase in the permeabilities of N-1, Ne-1, and Kr-1 depended on the number of pores formed. Because of recombination with fellow induced radicals, a part of the ion track formed by ion irradiation was closed again. The remarkable increase in the permeabilities of N-2 and Ne-2 were caused by the overlapping of the ion tracks at the higher fluence (10^{12} ions/cm^2). The overlapping of ion tracks at the higher fluence brought about a decrease in the yield of the radicals and enlarged the formed pore size. The overlapped pore was too large to recombine. Therefore, the pores formed by ion irradiation were fixed at high fluences. In the case of Xe ions, a higher P was obtained at the lower fluence, 3.0×10^{10} ions/cm^2. The energy of the Xe ion was very high, and it caused greater damage to the polymer chain network of PET. Therefore, the radicals could not recombine because of the enlargement of the pore size, and the formed pores were fixed.

Table III Permeability Coefficients for Various Gasses in Untreated and Heavy-Ion-Irradiated PET Membranes at 303 K

Sample[a]	Ion Beam	Fluence (ions/cm^2)	Permeability Coefficient[b] ($P \times 10^{10}$)			
			He	O_2	N_2	CO_2
PET	—	—	1.30	0.034	0.0045	0.16
N-1	$^{15}N^{3+}$	5.7×10^{10}	2.20	0.33	0.33	0.42
N-2	56 MeV	1.2×10^{11}	860.00	570.00	590.00	510.00
Ne-1	$^{20}Ne^{4+}$	8.7×10^{10}	2.20	0.40	0.40	0.47
Ne-2	75 MeV	1.7×10^{11}	390.00	180.00	200.00	180.00
Ar-1	$^{40}Ar^{8+}$	8.6×10^{10}	1.20	0.034	0.0045	0.16
Ar-2	150 MeV	1.3×10^{11}	1.20	0.037	0.0057	0.19
Kr-1	$^{84}Kr^{17+}$	6.0×10^{10}	1.60	0.19	0.17	0.26
Kr-2	322 MeV	1.0×10^{11}	4.30	0.91	1.40	1.33
Xe-1	$^{129}Xe^{23+}$	3.0×10^{8}	1.10	0.033	0.0047	—
Xe-2	450 MeV	3.0×10^{10}	480.00	230.00	210.00	230.00

[a] Thickness = about 12 μm.
[b] Unit = cm^3 (STP: Standard Temperature and Pressure) cm/cm^2 sec cmHg.

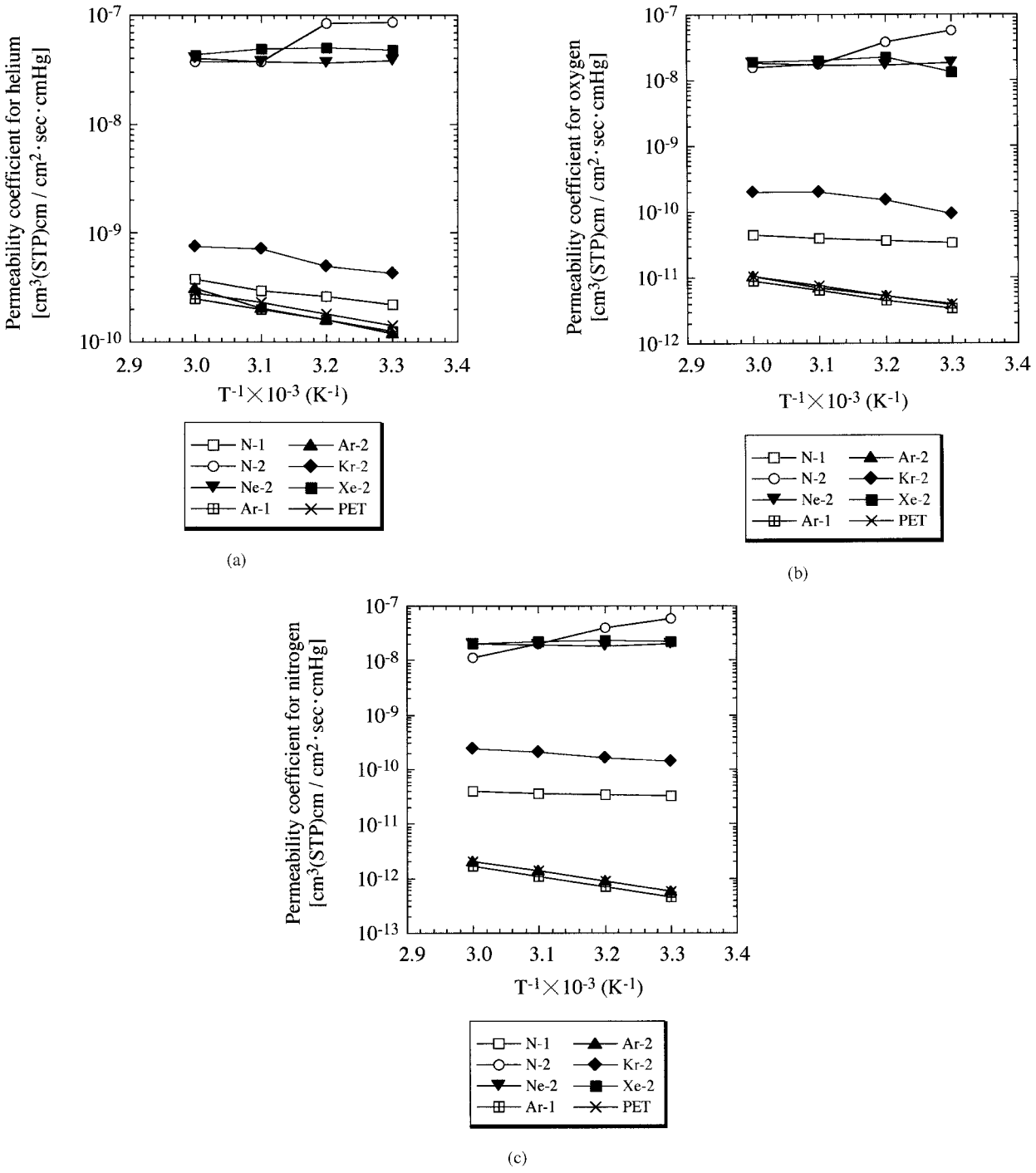

Figure 3 Temperature dependence of the *P*s for (a) helium, (b) oxygen, and (c) nitrogen in the PET membrane and ion-irradiated PET membranes.

Relationship of Activation Energy and Penetrant Gasses

The Arrhenius plots for various gasses with each sample were made to show their permeation behavior and are shown in Figure 3(a–c). These Arrhenius plots show that the permeation mechanism of the ion irradiation membrane were classified into at least three types. E_p was calculated from the eq. (1). The relationship between the E_p and the critical volume of the penetrant gasses is

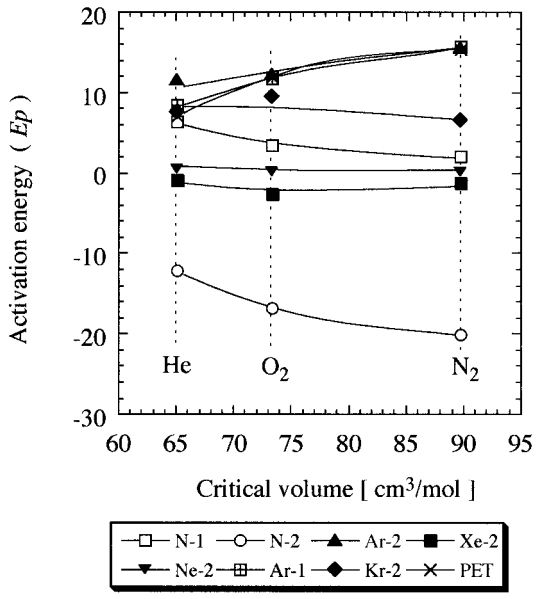

Figure 4 Relationship between the activation energy of each membrane and the critical volume of the penetrant gasses He, O_2, and N_2.

shown in Figure 4. The E_p of Ar-1 and Ar-2 exhibited values that were almost equivalent to that of PET. Moreover, the E_p of PET, Ar-1, and Ar-2 increased with an increase in the critical volume. The permeation behavior was determined exclusively by a solution–diffusion mechanism. However, N-2, Ne-2, and Xe-2, which had higher *P*s, as shown in Table III, had low activation energy values; especially those of N-2 and Xe-2 were negative. The E_p values of N-1 and Kr-2 were also very low. The level of E_p values decreased with the increase in the critical volume and was in reverse ratio to the size level of formed pore. That is to say, the lower E_p meant that penetrant gasses permeated through the larger pore. The E_p of N-1 and Kr-2, which showed a small change in permeability, also decreased with an increase in the critical volume. It was assumed that penetrant gasses permeated through the pores. Therefore, the effect of ion irradiation on the membrane depended on the energy, fluence, and kind of ion.

Knudsen Flow

When the size of the pores of the membrane is smaller than the mean free path of the gas molecules as noted previously, gas separation occurs. In the range of $r/\lambda < 1$ (where r is the radius of pore and λ is the mean free path), gas permeation of the penetrant molecules is considered to be Knudsen flow.[23] Gas molecules interact with the pore walls much more frequently than with other molecules. Low-molecular-weight gasses are able to diffuse more rapidly than heavier ones. In a vacuum state, the difference in the permeation rates of the two components is inversely proportional to the square root of the ratio of their molecular weights. In the case of the membranes, Knudsen flow was expressed by the following equation:

$$Q = \frac{4}{3} r\varepsilon \cdot \left(\frac{2RT}{\pi M}\right)^{1/2} \cdot \frac{(p_1 - p_2)}{\ell \cdot RT} \qquad (3)$$

where Q is the amount of permeant, ϵ is the porosity, M is the molecular weight of the penetrant, p_1 and p_2 are the pressures of the penetrant at the feed side and permeate side, respectively, and ℓ is the thickness of the membrane. The relationship between the permeability rate and the reciprocal of the square root of the gaseous molecular weight is shown in Figures 5–7. All membranes of Ar-1, Ar-2, and PET, as shown in the Figure 5, did not have penetrating pores. Thus, the gasses permeated through the polymer chain. As shown in Figure 7, the permeability rates of Ne-2 and Xe-2 were inversely proportional to the square root of the molecular weight of gasses. These results seemed to indicate that Knudsen flow occurred. Moreover, the relationships of the permeation behavior for Ne-1, Kr-1, and Kr-2 were also similar to the results for Ne-2 and Xe-2, as shown in Figure 7. The permeation behavior of

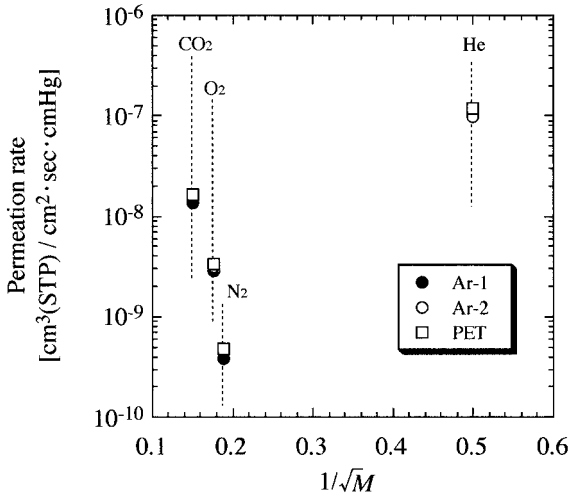

Figure 5 Relationship between the permeability rate and the reciprocal of the square root of the molecular weight of gasses at 303 K.

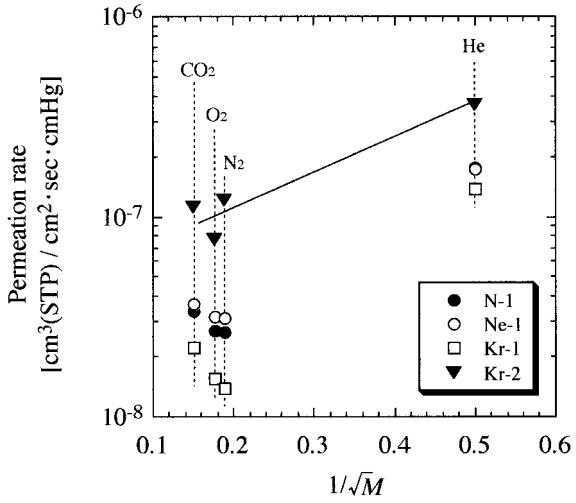

Figure 6 Relationship between the permeability rate and the reciprocal of the square root of the molecular weight of gasses at 303 K.

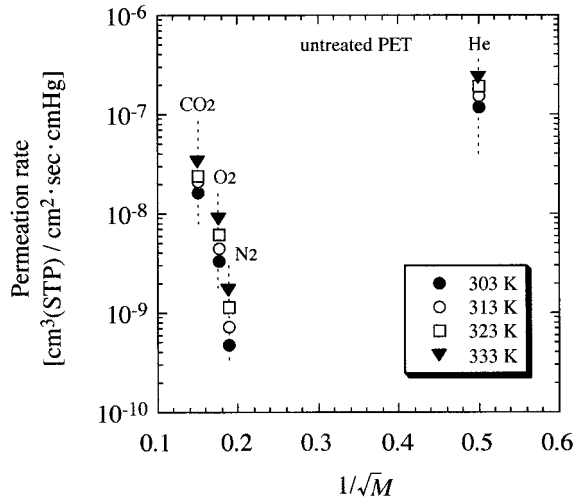

Figure 8 Effect of temperature on the relationship between the permeability rate and the reciprocal of the square root of the molecular weight of gasses on the untreated PET membrane.

N-1, Ne-1, and Kr-1, as shown in Figure 6, were nearly proportional to the reciprocal of the square root of the molecular weight of gasses. Thus, gas permeation takes place (1) through pores, (2) by permeation through the polymer chain, or (3) by a mixed mechanism. Regarding the permeation behavior of Kr-2, it seemed to show almost Knudsen flow. This assumes that pores were formed at the Knudsen flow level by heavy-ion irradiation. Our conclusion is that the permeation mechanism of heavy-ion-irradiated membranes is classified into three types as follows:

1. The radicals induced by ion irradiation were recombined, and all of the formed ion tracks were closed again. The penetrant gasses permeated by a solution–diffusion mechanism similar to that of the untreated PET membrane (PET, Ar-1, Ar-2, and Xe-1).
2. A part of the ion track formed by ion irradiation was closed again. The permeation

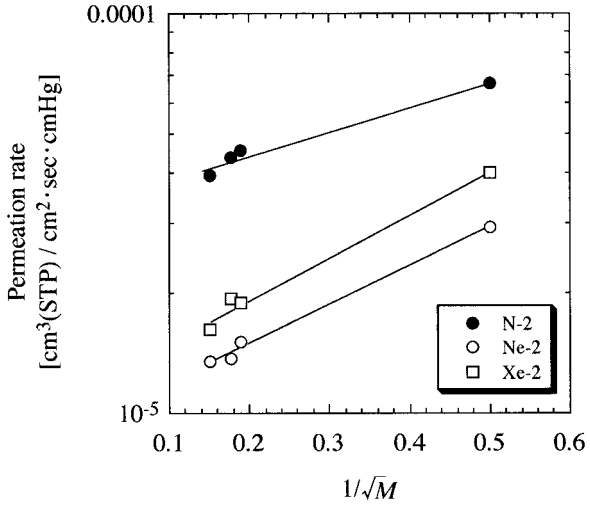

Figure 7 Relationship between the permeability rate and the reciprocal of the square root of the molecular weight of gasses at 303 K.

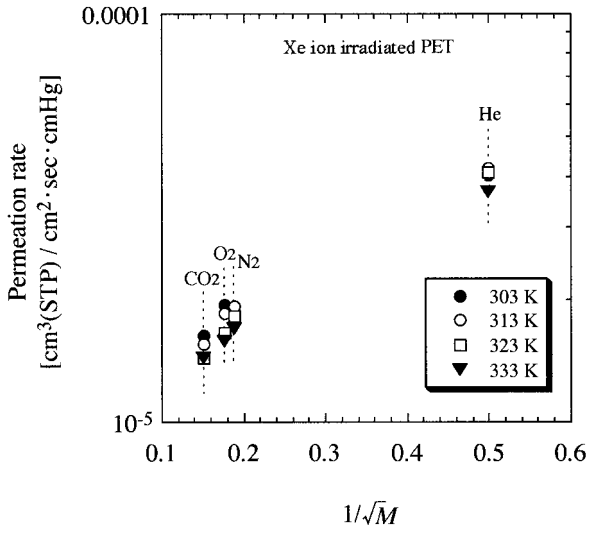

Figure 9 Effect of temperature on the relationship between the permeability rate and the reciprocal of the square root of the molecular weight of gasses on the Xe-ion-irradiated PET membrane.

was by both the solution–diffusion mechanism and the Knudsen flow (N-1, Ne-1, Kr-1, Kr-2).

3. The penetrant gasses preferentially permeated through the pore that was formed by ion irradiation (N-2, Ne-2, Xe-2).

Dependence of Temperature

The comparison of dependence of temperature between the Knudsen flow mechanism and the solution–diffusion mechanism was also investigated. The effects of the temperature in these relationships are shown in Figures 8 and 9. Figures 8 and 9 show the results for PET (as a solution–diffusion mechanism) and Xe-2 (as a Knudsen flow mechanism), respectively. In Figure 8, the permeability rate is shown to increase with increased temperature because the polymer chain motion became more active at the higher temperatures. The results of Figure 9 show a higher permeability rate at the lower temperature; however, they also seem to show permeation behavior through the pores.

Separation Factor of the Knudsen Flow

The theoretical separation factor of the Knudsen flow was defined by the following equation:

$$\alpha_{K\,A/B} = (M_B/M_A)^{1/2} \tag{4}$$

The theoretical value of the separation factor ($\alpha_{K\,A/B}$) of Knudsen flow and the ideal gas separation factor ($\alpha_{A/B}$) were calculated from eqs. (4)

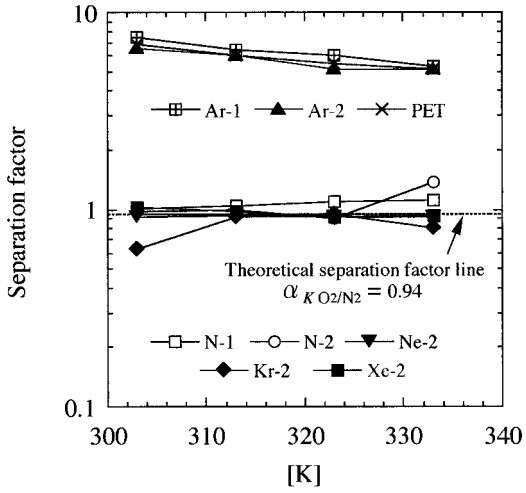

Figure 10 Temperature dependence of the ideal separation factor (P_{O2}/P_{N2}) in each PET membrane.

Table IV Ideal Separation Factors for O_2 over N_2 and CO_2 over N_2 in the Untreated and Heavy-Ion-Irradiated PET Membranes at Each Temperature

Sample	Ion Beam	Fluence (ions/cm^2)	Separation Factor							
			303 K		313 K		323 K		333 K	
			PO_2/PN_2	PCO_2/PN_2	PO_2/PN_2	PCO_2/PN_2	PO_2/PN_2	PCO_2/PN_2	PO_2/PN_2	PCO_2/PN_2
PET	—	—	6.90	34.00	6.00	29.00	5.50	21.00	5.10	19.00
N-1	$^{15}N^{3+}$	5.7×10^{10}	1.00	1.30	1.00	1.40	1.10	1.50	1.10	2.00
N-2	56 MeV	1.2×10^{11}	1.00	0.87	0.99	0.84	0.90	0.93	1.40	1.00
Ne-1	$^{20}Ne^{4+}$	8.7×10^{10}	1.00	1.20	—	—	—	—	—	—
Ne-2	75 MeV	1.7×10^{11}	0.91	0.89	0.93	0.88	0.92	0.85	0.92	0.86
Ar-1	$^{40}Ar^{8+}$	8.6×10^{10}	7.50	36.00	6.50	30.00	6.00	26.00	5.30	22.00
Ar-2	150 MeV	1.3×10^{11}	6.60	34.00	6.00	29.00	5.10	21.00	5.10	19.00
Kr-1	$^{84}Kr^{17+}$	6.0×10^{10}	1.10	1.60	—	—	—	—	—	—
Kr-2	322 MeV	1.0×10^{11}	0.63	0.93	0.91	0.98	0.95	1.05	0.81	1.10
Xe-1	$^{129}Xe^{23+}$	3.0×10^{8}	7.00	—	—	—	—	—	—	—
Xe-2	450 MeV	3.0×10^{10}	1.00	0.86	0.97	0.81	0.91	0.84	0.93	0.85

Theoretical separation factor of the Knudsen flow: $\alpha_{KO_2/N_2} = 0.94$, $\alpha_{KCO_2/N_2} = 0.80$.

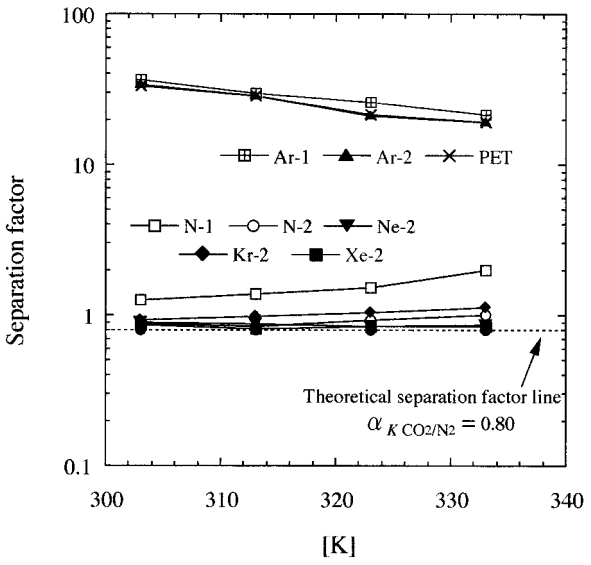

Figure 11 Temperature dependence of the ideal separation factor (P_{CO2}/P_{N2}) in each PET membrane.

and (2), respectively, and are shown in Table IV. The relationships between these separation factors of O_2/N_2 and CO_2/N_2 and temperature are shown in Figures 10 and 11, respectively. The ideal gas separation factor ($\alpha_{A/B}$) of all membrane in which the P increased because of heavy-ion irradiation nearly agreed with the line of the theoretical separation factor ($\alpha_{K\ A/B}$). When heavy ions penetrated the membrane by irradiation, therefore, the permeation behavior of the membrane showed Knudsen flow through the pores.

CONCLUSIONS

We carried out the modification of PET membranes by irradiation with various heavy ions and investigated the effect of heavy-ion irradiation on gas permeation. The d-spacing, density, and FTIR in the characterization spectrum did not show much difference between the untreated PET membrane and all of the irradiated PET membranes. In the fluence study, there was no difference between untreated PET membranes and Ar ion-irradiated membranes. However, membranes irradiated with other ions showed a remarkable change in gas permeation without a significant change in the polymer structure by ion irradiation. The permeation behavior of these membranes showed Knudsen flow because of the formation of pores by heavy-ion irradiation. Notably, the gas permeation of N-2, Ne-2, and Xe-2 increased remarkably on heavy-ion irradiation. As a result, the permeation behavior of these membranes in this study were classified into three types as follows: (1) a solution–diffusion mechanism, (2) the coexistence of solution–diffusion and Knudsen flow, and (3) a Knudsen flow mechanism.

In this study, the potential of damage to a PET membrane was in the following order for various ions:

$$^{129}Xe^{23+}(450\ MeV) > {}^{15}N^{3+}(56\ MeV) > {}^{20}Ne^{4+}(75\ MeV) > {}^{84}Kr^{17+}(322\ MeV) > {}^{40}Ar^{8+}(150\ MeV)$$

The effects of the ion irradiation on the gas-permeability properties of membrane were dependent on the type of ion irradiated, especially the energy and fluence of the ions. We believe that the control of gas permeability in a polymer membrane by ion irradiation is difficult. In the future, however, it is expected that many applications utilizing heavy-ion irradiation may emerge.

REFERENCES

1. Cacagno, L.; Percolla, R.; Foti, G. Nucl Instrum Methods Phys Res Sect B 1995, 95, 59.
2. Schnabel, W.; Klaumuenzer, Z. Radiat Phys Chem 1991, 37, 131.
3. Sasuga, T.; Kawanishi, S.; Nishi, M.; Seguchi, T.; Kohno, I. Radiat Phys Chem 1991, 37, 135.
4. Davenas, J.; Xu, M. A.; Boiteux, G.; Sage, D. Nucl Instrum Methods Phys Res Sect B 1989, 39, 754.
5. Said, M. A.; Balik, C. M. J Polym Sci Part B: Polym Phys 1988, 26, 1457.
6. Venkatesan, T.; Forrest, S. R.; Kaplan, M. L.; Murray, C. A.; Schmidt, P. H.; Wilkens, B. J. J Appl Phys 1983, 54, 3150.
7. Berndt, M.; Siegmon, G.; Beaujean, R.; Enge, W. Nucl Tracks Radiat Meas 1984, 8, 589.
8. Berndt, M.; Krause, J.; Siegmon, G.; Enge, W. Nucl Tracks Radiat Meas 1986, 12, 985.
9. Ogura, K.; Hattori, T.; Naito, T.; Nakano, K.; Takahashi, T. Nucl Tracks Radiat Meas 1993, 22, 921.
10. Yoshida, M.; Nagaoka, N.; Asano, M.; Omichi, H.; Kubota, H.; Ogura, K.; Vetter, J.; Spohr, R.; Katakai, R. Nucl Instrum Methods Phys Res Sect B 1997, 122, 39.
11. Koizumi, H.; Ichikawa, T.; Yoshida, H.; Shibata, H.; Tagawa, S.; Yoshida, Y. Nucl Instrum Methods Phys Res Sect B 1996, 117, 269.

12. Koizumi, H.; Ichikawa, T.; Yoshida, H.; Namba, H.; Taguchi, M.; Kojima, T. Nucl Instrum Methods Phys Res Sect B 1996, 117, 431.
13. Asano, M.; Yoshida, M.; Omichi, H.; Nagaoka, N.; Kubota, H.; Katakai, R.; Reber, N.; Spohr, R. Hosyasen 1996, 22, 61.
14. Yoshida, M.; Asano, M.; Safranj, A.; Omichi, H.; Spohr, R.; Vetter, J.; Katakai, R. Macromolecules 1996, 29, 8987.
15. Tamada, M.; Yoshida, M.; Asano, M.; Safranj, A.; Omichi, H.; Katakai, R.; Spohr, R.; Vetter, J. Polymer 1992, 33, 3169.
16. Nakagawa, T.; Hopfenberg, H. B.; Stannett, V. J Appl Polym Sci 1971, 15, 231.
17. Witchey-Lakshmahan, L. C.; Hopfenberg, H. B.; Chern, R. T. J Membr Sci 1990, 48, 321.
18. Nagai, K.; Nakagawa, T. J Membr Sci 1995, 105, 261.
19. Stannett, V. Diffusion in Polymers; Academic: London, 1968; p 41.
20. Nakagawa, T. Membrane Science and Technology; Marcel Dekker: New York, 1992; p 239.
21. Barrer, R. M. Trans Faraday Soc 1939, 35, 628.
22. Hama, Y.; Hamanaka, K.; Matsumoto, H.; Takano, T.; Kudou, H.; Sugimoto, M.; Seguchi, T. Radiat Phys Chem 1996, 48, 549.
23. Winston Ho, W. S.; Sirkar, K. K. Membrane Handbook; Van Nostrand Reinhold: New York, 1992; p 19.